Gaussian vs. Bessel light-sheets

Reidt, Sascha; Bango Da Cunha Correia, Ricardo; Donnachie, Mark; Weijer, Cornelis; MacDonald, Michael

Published in:
Proceedings of SPIE

DOI:
10.1117/12.2277324

Publication date:
2017

Document Version
Peer reviewed version

Gaussian vs. Bessel light-sheets: performance analysis in live large sample imaging

Sascha L. Reidt[a], Ricardo B. C. Correia[b], Mark Donnachie[a], Cornelis J. Weijer[b], Michael P. MacDonald*[a]

[a]Physics, School of Science and Engineering, University of Dundee, DD1 4HN Scotland; [b]School of Life Sciences, University of Dundee, DD1 5EH Scotland

ABSTRACT

Lightsheet fluorescence microscopy (LSFM) has rapidly progressed in the past decade from an emerging technology into an established methodology. This progress has largely been driven by its suitability to developmental biology, where it is able to give excellent spatial-temporal resolution over relatively large fields of view with good contrast and low phototoxicity. In many respects it is superseding confocal microscopy. However, it is no magic bullet and still struggles to image deeply in more highly scattering samples. Many solutions to this challenge have been presented, including, Airy and Bessel illumination, 2-photon operation and deconvolution techniques. In this work, we show a comparison between a simple but effective Gaussian beam illumination and Bessel illumination for imaging in chicken embryos. Whilst Bessel illumination is shown to be of benefit when a greater depth of field is required, it is not possible to see any benefits for imaging into the highly scattering tissue of the chick embryo.

Keywords: Lightsheet fluorescence microscopy, Bessel beams, DSLM, SPIM, chick embryos

1. INTRODUCTION

Light-sheet microscopy was selected as the Nature Method of the Year 2014 [1] and has become a go-to imaging technique in modern biology. It has shown itself to be of particular benefit for imaging larger more complex samples such as Zebrafish embryos, which themselves have the advantage of being relatively transparent when compared to other samples such as chicken embryos (another common model of human development). When imaging large samples, conventional Gaussian light-sheets are inherently limited by the trade-off between the beam waist and its depth of field, resulting in a non-uniform excitation across the field of view. Lately, Bessel and Airy lightsheets have been proposed because of their larger depth of field and their stability towards on-axis obstructions [2,3].

Recent studies describe the advantages of using Bessel beams and report an improved image quality, for example when imaging Arabidopsis root or when imaging cellular dynamics [4]. However, for the study of large scale and coordinated cell movements in embryonic development, a quantitative analysis of its performance is still missing. In our proceedings, we describe a novel application to Bessel beam light-sheet microscopy on large, living and highly scattering chick embryos and its potential use in answering important biological questions regarding coordinated cell movements, cell ingression and cell shape changes. We show that whilst using Bessel illumination can be of significant help when imaging thicker samples due to the increased depth of field, there is little or no benefit for overcoming light scattering during gastrulation in chick embryos.

In addition to beam shaping, there are other potential solutions to the challenge of scattering in lightsheet microscopy. One of those is multi-photon illumination, which allows for longer wavelength excitation to be used, hence reducing Rayleigh scattering. Another option is to use a multi-modal approach, where a lightsheet is used to excite an acoustic signal, which benefits from both the option to use longer wavelength illumination and the lack of scattering of the acoustic signal. We also discuss how it is important to consider the polarisation of excitation and emission light when using lightsheet microscopy as a result of the anisotropic nature of Rayleigh scattering when compared to Mie scattering.

*m.p.macdonald@dundee.ac.uk; phone +44 (0)1382 386988

1.1 Imaging in developmental biology

Imaging plays an important part in the study of cell behaviour during development. Controlled by internal or external signals, cells divide, migrate and differentiate to form an organism. These processes are studied using a variety of microscopy techniques, for example reviewed by Dormann [5]. Importantly Lightsheet microscopy is enabling the quantitative analysis of large developing embryos *in toto*. Frequently applied to imaging of zebrafish and fruit flies, it was used to produce their *digital embryos* and has advanced the understanding of their development. The technique is also suitable to studying the development of higher organisms, as demonstrated on the primitive streak formation of the chick embryo [6]. The primitive streak formation is a part of the gastrulation stage in embryonic development, and initiates the germ layer formation. As such, it is crucial for the successful development of an organism, but its main driving forces and their biochemical origins are still unclear and remain a widely researched topic.

1.2 Benefits of lightsheet microscopy

Lightsheet microscopy describes a technique based on laser lightsheet illumination with an imaging axis oriented orthogonally to the lightsheet. The imaging geometry has the advantage that the sample is optically sectioned, minimising contributions from outside of the focal plane of the detection axis. This results in improved axial resolution as well as more efficient fluorescence excitation, which reduces photodamaging and photobleaching rates. In addition, images are acquired in widefield, allowing high-speed image acquisition. The high spatio-temporal resolution combined with low photobleaching rates makes lightsheet microscopy an ideal technique for live imaging of embryonic development [7].

2. GAUSSIAN BEAM ILLUMINATION

It is a rule of thumb that the simpler a technology is, the more robust and effective it is. Lightsheet microscopy is no exception to this and high quality imaging can be obtained using very simple setups, even to the extent of using scattering for contrast instead of fluorescence. In this section, we describe how a simple Gaussian set up can yield high quality images, using scattering and fluorescence and additionally highlight the important role that polarisation plays when imaging a sampled orthogonally to the illumination axis.

2.1 Digitally Scanned Lightsheet microscopy and confocal scanning acquisition

Apart from refractive optical elements like cylindrical [8] or Powell lenses [9], laser lightsheets can also be generated using scanners [10]. In our setup, the beam is scanned with a galvanometric mirror in one axis, and projected into the sample using a scan lens, a tube lens and a 10x water dipping illumination objective (NA 0.3). For imaging of the flat and large chick embryos, the lightsheet is oriented at 45 degrees to the horizontal, and the embryo is moved through the lightsheet on a motorised translation stage. The height of the stage is continuously adjusted to keep the surface of the embryo in the focus of the lightsheet. The signal of each optical section is collected with another 10x water dipping objective (NA 0.3) to construct three-dimensional images of the chick embryo development. The chick embryos are transgenic, labelled with membrane-bound green fluorescent proteins and mounted in liquid culture. With this system, the development of chick embryos with a size of several millimetres can be imaged at cellular resolution over long periods of time, with a temporal resolution of about 3 minutes per full time point (complete 3D stack of data). Further details on the basic optical setup and mounting technique can be found elsewhere [6].

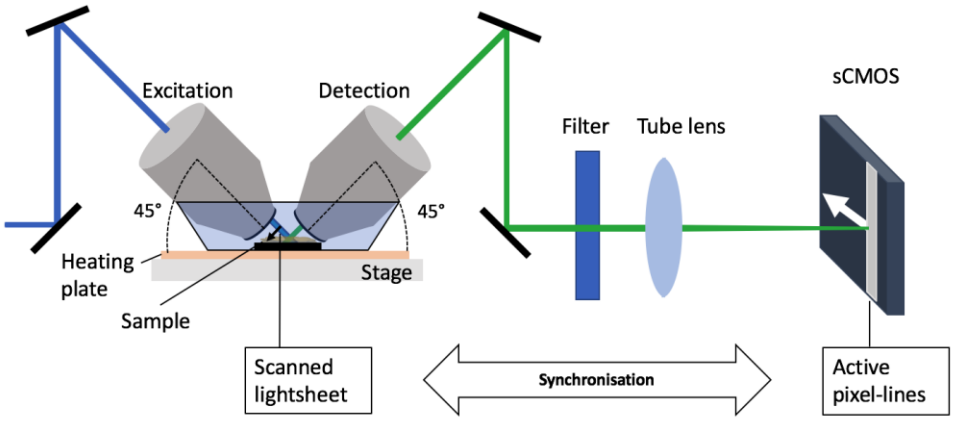

Figure 1. Digitally scanned lightsheet microscopy for chick embryo imaging with confocal line acquisition.

Biological samples are often highly scattering, and lightsheet images of chick embryos suffer from noise caused by deflected excitation and emission photons. The influence of the scattering can be reduced by using a confocal line acquisition technique [11]. Modern sCMOS cameras offer the possibility of a line-by-line readout mode of the camera chip, which can be synchronised with the scanning of the excitation laser lightsheet as shown in Figure 1. This acquisition type blocks out-of-focus photons, reducing the noise caused by scattering.

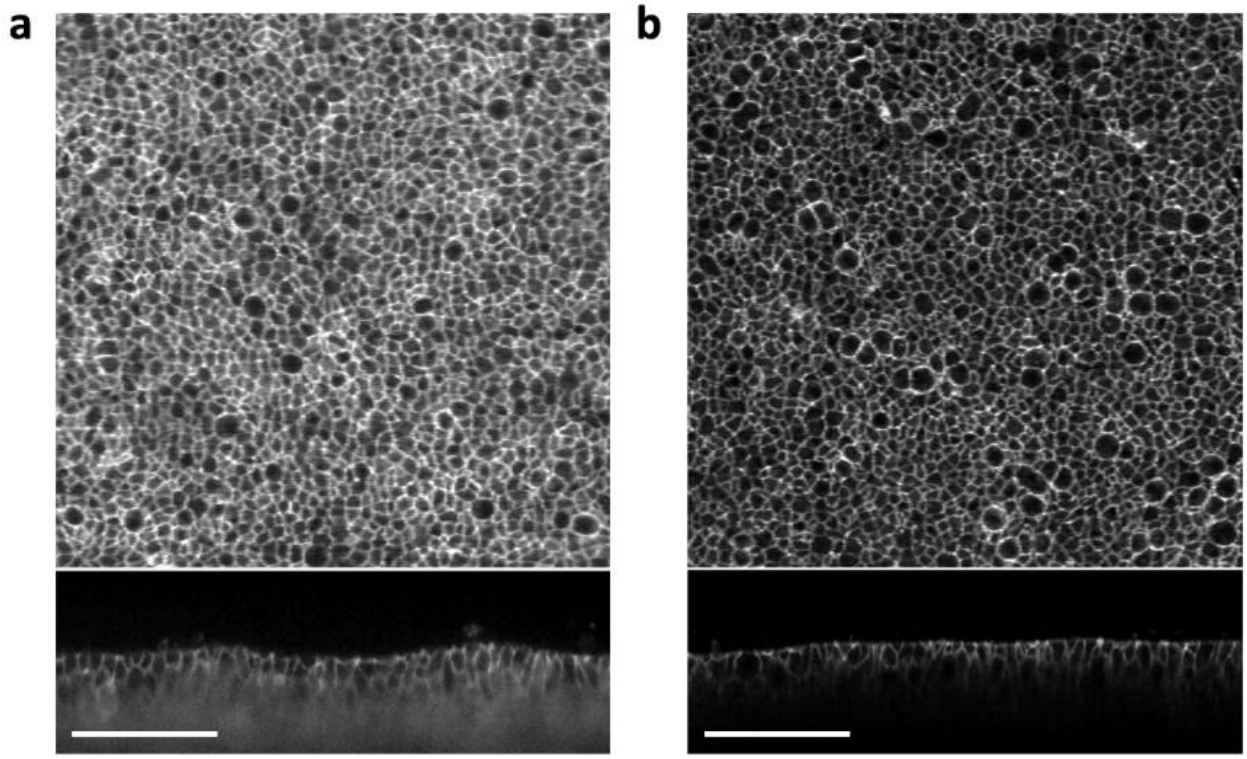

Figure 2. Normalised Gaussian lightsheet images of the epiblast of a living chick embryo at an early stage of development, with the tissue surface on top and a cross-section below. (a) Gaussian rolling shutter acquisition. (b) Gaussian confocal line acquisition. Scale bars are 100 µm.

Figure 2 shows representative images of the surface of the epiblast cell layer of a living chick embryo. From the three-dimensional data, the cell surface of the epiblast is calculated by projecting the first grey values higher than a certain threshold to a plane. Even though the noise could be reduced and the image quality seemingly improved, this acquisition mode had limited effects on the amount of information that could be extracted from the images. In the presented system, the line readout mode of the camera is still considerably slower (15 Hz) than the standard rolling shutter (100 Hz), and synchronising it to the laser scanner presents a challenging alignment task.

2.2 Scattering for contrast

Scattering is not always a problem in imaging and can be used to give the contrast needed to form an image. Lightsheet imaging is no exception to this [12]. In fact, it is possible to combine scattering imaging along with fluorescence imaging to get dual contrast images of chick embryos. These images can be acquired sequentially, or by using dichroic mirrors to split the wavelengths.

Figure 3 shows an example of the co-registration of scattering and fluorescence contrast. Due to the orthogonal geometry of the system, the scattering contrast is highly dependent on the polarisation. In this case, most of the scattered light comes from a direct reflection on a structure called the vitelline membrane, which spans the embryo (Figure 3a). These reflections can be filtered by using a linear polarised-analyser configuration, which allows us to image contrast from the sub-germinal space of the embryo (Figure 3b). Knowing the region of the sub-germinal space can then provide the basis for further experiments, for example with an inducible GFP chick embryo line.

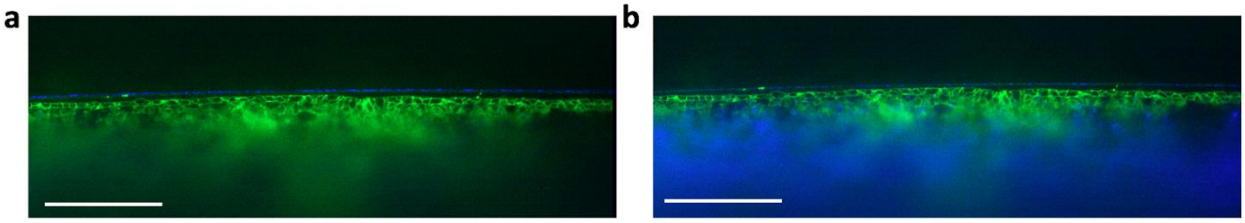

Figure 3. Dual contrast lightsheet imaging of the epiblast of a living chick embryo at an early stage of development. Fluorescence coloured in green, scattering contrast coloured in blue. (a) No polarization control. (b) Cross-polarised analysis. Scale bars are 200 μm.

2.3 The importance of considering polarisation

The polarisation of the light doesn't only influence specular reflections, but also more generally elastic scattering. Single elastic Mie scattering is not highly polarising, but Rayleigh scattering events *are* polarising and deflect perpendicular polarised light into the orthogonal direction. This effect becomes important in orthogonal imaging of scattering contrast, and can be utilised to reduce background noise by using a linear polariser in the illumination axis and a linear analyser in the detection axis [13]. As a demonstration of this effect, we used a phantom consisting of reflecting polystyrene microspheres with a size of 100 μm, immersed in a highly scattering mixture of 0.1 weight/volume gelatine and distilled water (Figure 4).

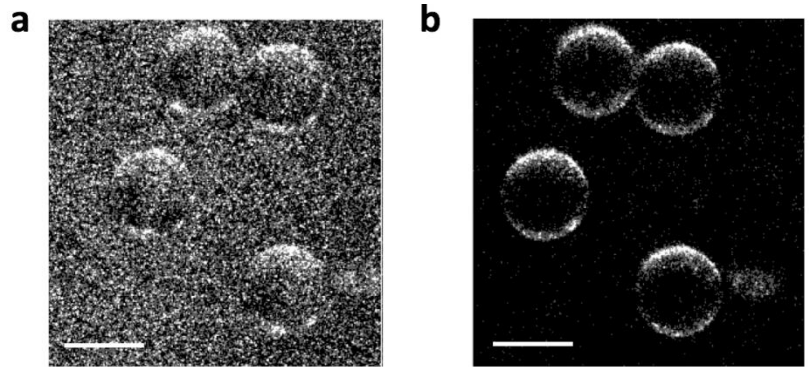

Figure 4. Scattering contrast of reflecting 100 μm microspheres immersed in gelatine. (a) Perpendicular polarised illumination without an analyser. SNR = 1.7. (b) Parallel polarised illumination with parallel polarised analysis to reduce orthogonal Rayleigh scattering noise. SNR = 68.5. Scale bars are 100 μm.

Figure 4 highlights the importance of polarisation control in lightsheet imaging of scattering contrast, caused by a combination of the polarisation by scattering and the diffusion of polarisation in highly scattering media. These results motivate further experiments, for example co-registration of multiple scattered wavelengths as an additional contrast mechanism, coming from the absorption spectrum of a sample as well as the strong wavelength dependency of Rayleigh scattering.

3. BESSEL BEAM ILLUMINATION

When looking for a solution to scattering in samples, an obvious approach is to use a beam with self-healing capabilities such as a Bessel beam. Another benefit of a Bessel beam is that it is essentially non-diffracting, such that an improved Rayleigh range is possible. Bessel beams are by no means the only form of excitation that can improve image quality in the presence of scattering and absorption, with Airy beams also capable of significant improvements in certain circumstances [3].

In this work, we use Bessel beams to compare the performance of non-diffracting beams against conventional Gaussian imaging. Bessel beams are interference patterns formed by plane waves travelling on a cone. Thus, quasi-Bessel beams can be generated by applying conical phase shifts to a Gaussian beam, using an axicon or a spatial light modulator. Here, a spatial light modulator is used in a configuration described by Fahrbach [14]. We implement the spatial light modulator in a separate beam path using flip mirrors to allow comparison to the original Gaussian illumination. In the secondary optical path, the beam is expanded, and the polarisation is adjusted with a half-wave plate. It is then reflected off the liquid crystal display of the spatial light modulator and modulated with a programmable phase shift. Higher diffraction orders and unmodulated light is blocked with a spatial filter, and only the modulated beam is used for imaging. Such a setup gives great flexibility and allows for the optimisation of the beam parameters to suit specific imaging applications. However, fluorescence excitation with Bessel beams requires additional measures due to the contributions of the concentric side lobes of a Bessel beam to the acquired image.

3.1 Bessel confocal

Imaging with a Bessel beam has the effect of a convolution of each pixel in the planes orthogonal to the lightsheet with the corresponding Bessel profile. In practice, a deconvolution of the images with the full Bessel profile did not significantly improve the image quality. However, contributions of the Bessel beam side lobes can be reduced with the confocal line acquisition described above. Synchronising the scanned Bessel beam with the line readout of the camera is equivalent to a one-dimensional masking. The line width is chosen to be in the range of the diameter of the central core (5 Pixels wide, equivalent to 3.25 μm), and smaller than the first Bessel ring. This mask blocks the longitudinal parts of the side lobe contributions, and makes the effective imaging equivalent to imaging with multiple parallel lightsheets.

3.2 Deconvolution

The resulting confocal Bessel images can now be deconvolved for a reduction of the remaining noise coming from the transversal part of the side lobes. The point spread function of the system is measured by reflecting the excitation Bessel lightsheet in the sample chamber using a mirror, and acquiring an image of its cross-section in the confocal mode. The original image stack at 45 degrees is transformed into individual sections orthogonal to the lightsheet. To reduce computation time, these two-dimensional sections are deconvolved on the GPU with the measured point spread profile, using an adapted version of the Richardson-Lucy algorithm implemented in MATLAB.

3.3 Comparison with Gaussian illumination, scattering

Deconvolution of the images acquired with the confocal Bessel beam gave good image quality on the surface of the epiblast, showing that the side lobe noise can be suppressed efficiently. However, the Bessel beam did not significantly improve the penetration depth into the highly scattering tissue of the chick embryo (Figure 5).

The cross-sections of Figure 5a show that there is a higher intensity deeper inside the tissue without the confocal-line acquisition mode. As a measurement for sharpness, the mean norm of the greyscale gradient was calculated as a function of the penetration depth. However, the gradient sharpness is dominated by high frequencies as are, for example, present in diffused noise, and therefore not a suitable metric to quantify image quality in this case. Thus, a frequency based *useful contrast ratio* was calculated, defined as the intensity in the useful frequency range (2.5 – 10 µm) divided by the intensity of the remaining frequencies. The useful contrast of the standard Bessel beam is never greater than one, suggesting that the signal intensity never exceeds the noise. The normal Gaussian and the confocal Bessel show good contrast on the surface with a quick decay. Both the confocal Gaussian and the deconvolved confocal Bessel appear to give slightly greater penetration depths into the cell layer. However, the image quality is not good enough for further processing and for an analysis of cell shape changes, ingression or migration.

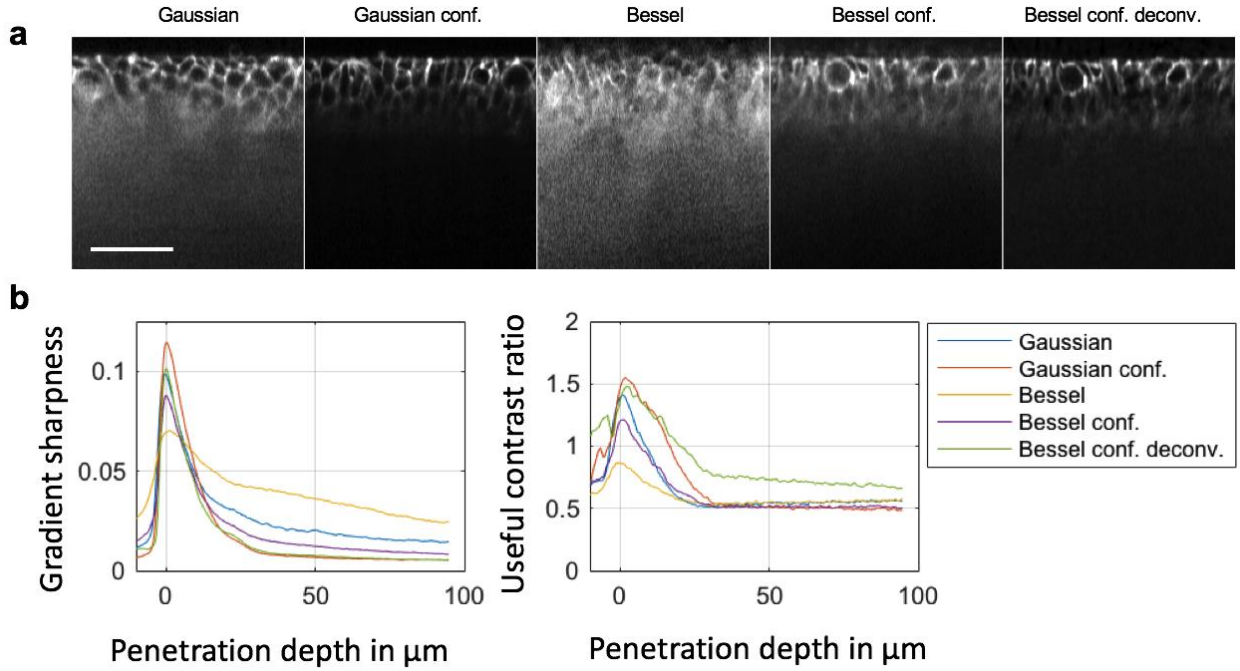

Figure 5. Comparison of the penetration depth into a region near the primitive streak of a living chick embryo for five imaging modes. (a) Raw cross-section. (b) Sharpness estimation as a function of the penetration depth. Scale bar is 100 µm.

3.4 Comparison with Gaussian illumination, depth of field

The extended depth of field of the Bessel beam became useful for imaging of the later stages of chick embryo development. At these stages, the embryo becomes larger, more transparent and features a high curvature on the surface. The depth of field of the Gaussian is not large enough to keep the whole structure in focus, and the Bessel beam can help to image a larger part of the embryo. Figure 6 shows two representative cross-sections of the blood vessel formation in the living chick embryo, where the image quality of the Bessel beam exceeded the one of the Gaussian beam.

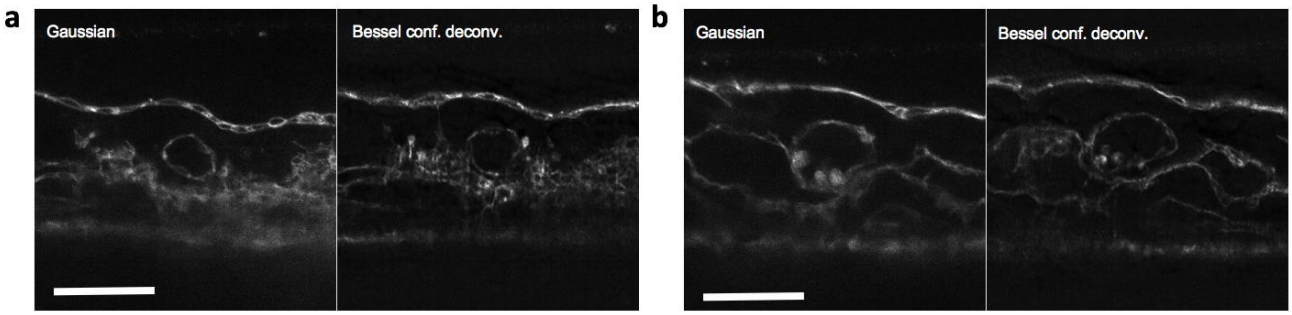

Figure 6. Two examples (a, b) of the blood vessel formation in a later stage chick embryo, acquired using the original Gaussian illumination and the deconvolved confocal Bessel mode. Scale bars are 100 μm.

4. OPTOACOUSTIC BESSEL BEAM ILLUMINATION

It is clear that though Bessel illumination is of real benefit for increasing the depth of field of a lightsheet microscope, it is less clear that they are of any real benefit when there is scattering right across the illumination wavefront. One solution to scattering which has been gaining traction in the last decade is opto-acoustic imaging. Here we combine lightsheet excitation with opto-acoustic imaging to show how the self-healing nature of Bessel beams can help significantly in the presence of localised absorption and for gaining a stronger signal through the full depth of a sample.

In a proof-of-principle experiment, we used a nanosecond pulsed Nd:YAG laser at a wavelength of 532 nm with a pulse repetition rate of 15 Hz. The beam shaping optics are interchangeable, comprising of either a 5x objective lens for a Gaussian focus or a 5˚ axicon for a Bessel beam. The two beam profiles are imaged with a telescope into a water chamber. The samples are mounted on a three-dimensional translation stage, and the acoustic signals are measured with a home-made cylindrical PVDF transducer. The transducer is placed on the extended axis of the beam behind a diffusively reflecting sheet. The acoustic signal is amplified, bandpass filtered and measured with an oscilloscope, which is triggered by the laser driver. In later experiments, the illumination laser will be scanned with a galvanometric mirror to generate a lightsheet, and the acoustic signals will be acquired with a linear array transducer.

4.1 Increased signal at depth in scattering samples

The depth of field of the two beams was tested by translating an absorbing wire along the direction of the illumination beam, and measuring the opto-acoustic signal at each position. The intensity of the laser is normalised to give the same peak acoustic signal, because the acoustic signal is proportional to the fluence in the sample, which is the limiting factor in biomedical imaging due to safety considerations. Figure 7 shows the acoustic signals during translation of the absorber. With Gaussian illumination, the signal peaks after around 3 mm, before it decays. It falls below the noise level at approximately 12 mm. The Bessel illumination gives a constant amplitude over the entire distance of 15 mm, showing the capability of the Bessel beam to increase the signal at depth.

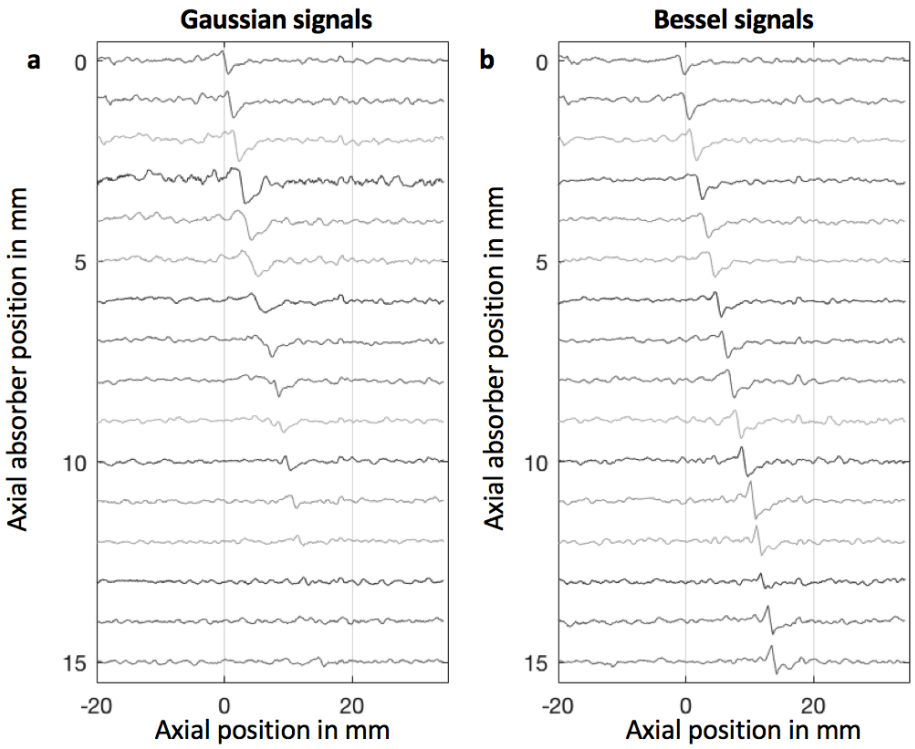

Figure 7. Averaged opto-acoustic signals from a translated absorber. The temporal signals are acquired with the transducer and converted to the spatial scale using the known speed of sound in water. (a) Gaussian beam. (b) Bessel beam.

4.2 Self-healing

Another phantom, consisting of a series of absorbing wires, was scanned through the illumination beam to obtain a series of amplitude scans for image formation. The absorbers are placed at a distance of 10 mm, with the first two still within the useful depth of field of the Gaussian beam.

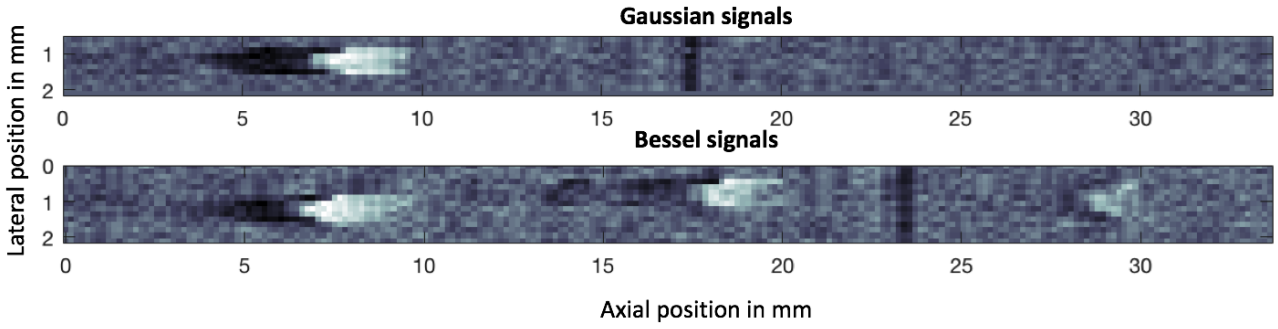

Figure 8. A series of amplitude scans to image three serial absorbers in the phantom. Gaussian beam on top and the Bessel beam below with the illumination coming from the left.

The normalised amplitude images are presented in Figure 8. The intensity of the Gaussian beam is absorbed by the first wire, which gives a strong photoacoustic signal. The two following absorbers could not be detected because they are shadowed by the first absorber. The Bessel beam is also absorbed at the first absorber, but the central core reconstructs from the side lobes, giving another signal from the second and third absorber. This suggests that the Bessel beam is more robust when it encounters localised obstructions, as would be expected. Together with the extended depth of field, this makes Bessel beams an interesting alternative to Gaussian beams for imaging of complex samples in opto-acoustics.

5. MULTIPHOTON LIGHTSHEET MICROSCOPY

One of the benefits of optoacoustic imaging is that it allows for the use of longer wavelength excitation. However, that improvement can also be made in LSFM, by using 2-photon illumination. Such an approach also allows for a small increase in resolution, but this is balanced by the increased laser power needed to obtain a signal resulting in much higher phototoxicity. In this section we show results for 2-photon lightsheet imaging so that they may be compared to the conventional approach described in section 3.

5.1 Results for two photon illumination

A tuneable femtosecond Ti:Sapphire laser is co-aligned with the original 488 nm illumination described in section 3. The optimum wavelength, often a trade-off between the efficiency of the laser and the efficiency of the fluorescence excitation, is found to be around 900 nm. Chick embryos featuring a primitive streak are imaged at 488 nm and 900 nm excitation. As presented in Figure 9, the higher wavelength and the square-dependency of the signal on the excitation intensity lead to a better performance in the scattering tissue. However, the low efficiency of 2-photon excitation requires a high photon flux in the embryo, which leads to photobleaching and phototoxicity when imaging over prolonged periods of time.

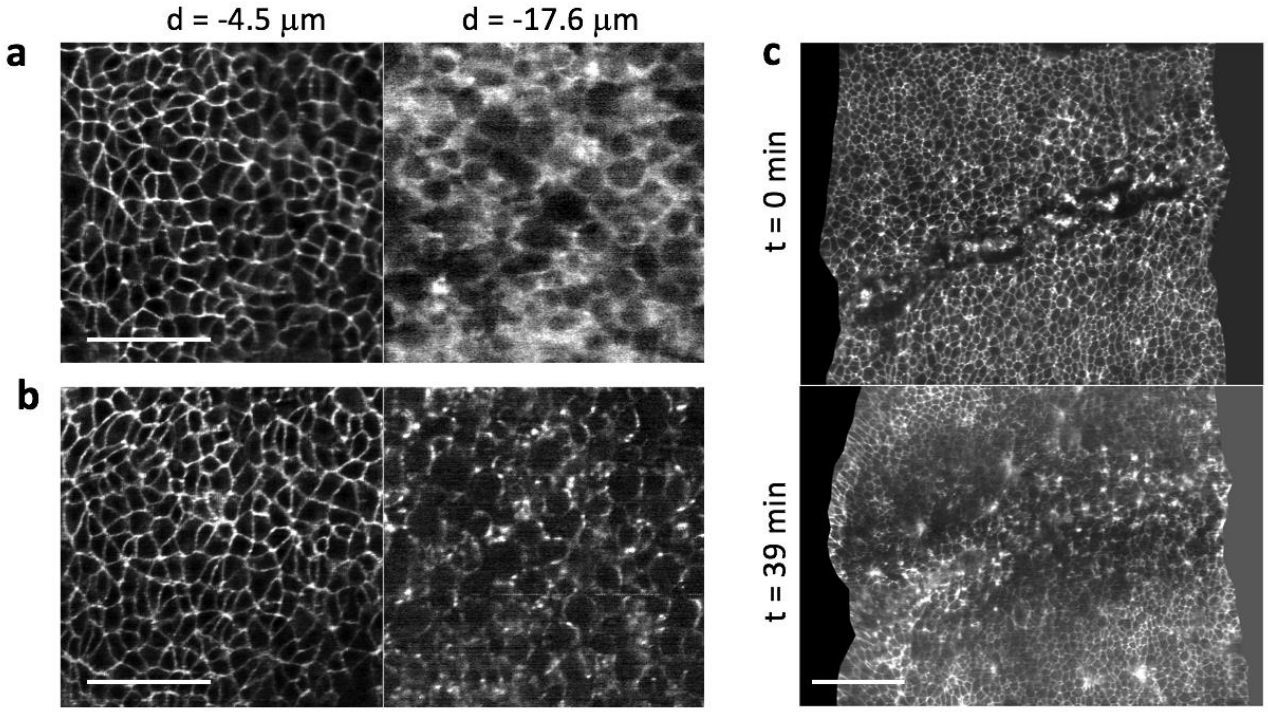

Figure 9. Epiblast of live chick embryo imaged with 2-photon lightsheet microscopy. (a) Cell layer at two different depths, excited with 488 nm. (b) Cell layer at two different depths, excited with 900 nm. (c) Two selected normalised time-points acquired at 40x showing phototoxic effect after 39 min. Scale bars are 100 μm.

6. CONCLUSIONS/DISCUSSION

In this work we have quantitatively assessed Bessel beam illumination over Gaussian illumination for imaging in large and complex biological samples. In addition, we have introduced other approaches to reducing or overcoming scattering, including using opto-acoustics and multi-photon microscopy. Despite being able to give the anticipated increase in depth of focus, Bessel illumination did not give a significant improvement in the ability to image within highly scattering samples. This is most likely due to the scattering taking place across the entirety of the Bessel beam's

conical wavefront, such that its ability to self heal is compromised. However, if used in opto-acoustic mode, we again see the benefits of the non-diffracting nature of a Bessel beam with an opto-acoustic signal obtainable through a much greater depth than with a Gaussian beam, making it more suited to lighsheet imaging. Additionally, as one would expect, in the presence of localised absorbers a Bessel beam was able to give a marked improvement in imaging through its ability to self heal. Finally, to complete the picture we have shown that 2-photon excitation, through the ability to use longer wavelength excitation, delivers higher quality images more deeply within the chick embryo. This should allow for tracking of cells within the forming mesendoderm of the embryo. However, the greatly increased laser fluence required to achieve 2-photon excitation, when compared to linear fluorescence excitation, leads to a greatly increased phototoxicity, such that sample lifetime is reduced significantly.

In summary, where imaging of only the epiblast of an early stage chick embryo is required, simple Gaussian illumination is the best approach to take. However, for later stages in embryo development, where the surface becomes more contorted (less flat) beyond the point where auto-focus type height adjustment of the sample can make the necessary compensation, the added depth of field afforded by Bessel illumination can be of measureable benefit. We have also seen that a Bessel beam could be of real benefit for increasing signals at depth within opto-acoustic imaging and for imaging behind localised absorbers. Finally, we have shown that the only effective way to gain imaging deeper within a sample in a purely optical approach is to use multiphoton illumination, but that this comes at the cost of increased phototoxicity.

REFERENCES

[1] Method of the Year 2014. Nat. Methods 12, 1–1 (2014).

[2] Gao, L., Shao, L., Chen, B.-C. & Betzig, E., "3D live fluorescence imaging of cellular dynamics using Bessel beam plane illumination microscopy," Nat. Protoc. 9, 1083–1101 (2014).

[3] Vettenburg, T. et al., "Light-sheet microscopy using an Airy beam," Nat. Methods 11, 541–544 (2014).

[4] T. Meinert, O. Tietz, K.J. Palme & A. Rohrbach, "Separation of ballistic and diffusive fluorescence photons in confocal Light-Sheet Microscopy of Arabidopsis roots," Scientific Reports 6, Article number: 30378 (2016)

[5] Dormann, D. & Weijer, C. J., "Imaging of cell migration," EMBO J. 25, 3480–93 (2006).

[6] Rozbicki, E. et al., "Myosin-II-mediated cell shape changes and cell intercalation contribute to primitive streak formation," Nat. Cell Biol. 17, 397–408 (2015).

[7] Tomer, R., Khairy, K. & Keller, P. J., "Shedding light on the system: Studying embryonic development with light sheet microscopy," Curr. Opin. Genet. Dev. 21, 558–565 (2011).

[8] Voie, A. H., Burns, D. H. & Spelman, F. A., "Orthogonal-plane fluorescence optical sectioning: three-dimensional imaging of macroscopic biological specimens," J. Microsc. 170, 229–236 (1993).

[9] Saghafi, S., Becker, K., Hahn, C. & Dodt, H.-U., "3D-ultramicroscopy utilizing aspheric optics," J. Biophotonics 7, 117–125 (2014).

[10] Keller, P. J. & Stelzer, E. H. K., "Quantitative in vivo imaging of entire embryos with Digital Scanned Laser Light Sheet Fluorescence Microscopy," Curr. Opin. Neurobiol. 18, 624–632 (2008).

[11] Baumgart, E. & Kubitscheck, U., "Scanned light sheet microscopy with confocal slit detection," Opt. Express 20, 21805–21814 (2012).

[12] Yang, Z., Downie, H., Rozbicki, E., Dupuy, L. X. & MacDonald, M. P., "Light Sheet Tomography (LST) for in situ imaging of plant roots," Opt. Express 21, 16239–16247 (2013).

[13] Reidt, S. L., O'Brien, D. J., Wood, K. & MacDonald, M. P., "Polarised light sheet tomography," Opt. Express 24, 11239–11249 (2016).

[14] Fahrbach, F. O., Gurchenkov, V., Alessandri, K., Nassoy, P. & Rohrbach, A., "Light-sheet microscopy in thick media using scanned Bessel beams and two-photon fluorescence excitation," Opt. Express 21, 13824–13839 (2013).